Annales Societatis Geologorum Poloniae (2018), vol. 88: 303–319 doi: https://doi.org/10.14241/asgp.2018.020

SOLUTION-COLLAPSE BRECCIAS IN THE UPPER OLENEKIAN–LADINIAN SUCCESSION, TATRA MTS, POLAND

Piotr JAGLARZ & Tomasz RYCHLIŃSKI

Jagiellonian University, Faculty of Geography and Geology, Institute of Geological Sciences, Gronostajowa 3a; 30-387 Kraków, Poland;
e-mails: piotr.jaglarz@uj.edu.pl, tomasz.rychlinski@uj.edu.pl

Jaglarz, P. & Rychliński, T., 2018. Solution-collapse breccias in the upper Olenekian–Ladinian succession, Tatra Mts, Poland. *Annales Societatis Geologorum Poloniae,* 88: 303–319.

Abstract: The upper Olenekian–Middle Triassic succession of the Tatricum domain (Central Western Carpathians, southern Poland) includes a few horizons of breccias, which are intercalated with early-diagenetic dolostones. On the basis of macroscopic and microscopic (including cathodoluminescence) observations, the paper presents a new interpretation of the genesis of the breccias and their diagenetic history. The rocks studied range from monomictic, cemented mosaic packbreccias to chaotic, unsorted, monomictic, particulate rubble floatbreccias. The processes that preceded the formation of the breccias encompassed the precipitation of evaporites and the early-diagenetic dolomitization of lime muds. The solution-collapse breccias were formed during episodes of cyclic sediment emersions in the upper Olenekian and Middle Triassic, as the result of gradual sediment collapse after karstic dissolution of the intercalated evaporites. After the brecciation process, during diagenesis the rocks were subjected to cementation by sulphate minerals and next, to multi-stage dolomitization. Later tectonic processes led to fracturing and even re-brecciation of the previously formed solution-collapse breccias.

Key words: Palaeokarst, evaporites, solution breccia, dolomitization, diagenesis, Tatricum, Triassic, Western Carpathians

Manuscript received 23 February 2018, accepted 20 December 2018

INTRODUCTION

Breccias are rocks composed of angular clasts, associated with a matrix and/or cements. Studies of sedimentary and diagenetic breccias provide information about the sedimentary environment or post-depositional (e.g., karst or tectonic) processes (Blount and Moore, 1969).

Solution-collapse breccias are among the most significant categories of carbonate breccias, usually accompanied by complexes of shallow-water carbonates, deposited under hypersaline conditions (e.g., Friedman, 1997). They are formed as the result of karst processes, when dissolution and washing out of evaporite minerals leads to the collapse of the overlying sediments (Beales and Hardy, 1980; Friedman, 1997). Such breccias are the most common evidence of evaporite dissolution. However, the processes that lead to their formation might occur at different stages of diagenesis (e.g., Swennen *et al.,* 1990; Pomoni-Papaioannou and Carotsieris, 1993; Scholle *et al.,* 1993; Karakitsios and Pomoni-Papaioannou, 1998; Pomoni-Papaioannou and Karakitsios, 2002; Eliassen and Talbot, 2005).

This paper focuses on a few horizons of dolostone breccias in the upper Olenekian (Myphoria Beds) and Middle Triassic carbonate succession of the Tatricum domain in the Tatra Mts. The formation mechanism of these breccias is still the subject of debate. Some authors (Kotański, 1954, 1956) interpret them as wave-inducted, intraformational breccias or transgressive (basal, cliff) breccias, while the others suggest a tectonic origin for them, but do not exclude the possibility that some of them are sedimentary breccias, subsequently modified by tectonic processes (Jurewicz, 2005).

This paper presents a new interpretation of the brecciation mechanism. The conditions of evaporite dissolution, sediment collapse, cementation of breccias, their further diagenetic transformation and the relative time of these processes are also discussed in detail.

GEOLOGICAL SETTING

General setting

The Tatra Mountains are the most northerly situated massif of the Central Western Carpathians. The Tatra massif is composed of a Palaeozoic crystalline core and a Mesozoic sedimentary cover. The crystalline core (granitoids and metamorphic rocks) was formed during the Variscan orogeny (Burchart, 1968; Janák, 1994), while the sedimentary cover was folded and thrusted during the Subhercynian phase of the Alpine orogeny (Kotański, 1961). The Mesozoic sedimentary cover is composed of the High-Tatric autochthon, which directly covers the crystalline core and the system of tectonic units, grouped into the High-Tatric and Sub-Tatric nappes. The High-Tatric autochthon (locally parautochthon) in turn is covered by the Czerwone Wierchy (lower) and the Giewont (upper) nappes (the High-Tatric allochthon; Dumont *et al*., 1996). The High-Tatric Unit (the High-Tatric autochthon and the High-Tatric allochthon) is overlain by the Lower Sub-Tatric (Krížna) Nappe, which in turn is overlain by the Upper Sub-Tatric (Choč) Nappe (Fig. 1A). All the tectonic units are discordantly covered by Eocene conglomerates and limestones, which are the older part of the so-called Inner Carpathian Palaeogene (Roniewicz, 1969; Soták, 2010). The Tatra massif was uplifted during the early Neogene (Bac-Moszaszwili, 1995).

The High-Tatric Unit (Permian–lower Turonian) represents the Tatricum palaeotectonic-facies domain (Andrusov *et al.*, 1973; Wieczorek, 2000). In the Triassic period, the Tatricum was the Carpathian part of the Western Tethys on the southern edge of the North European Platform (Michalík, 1993, 1994), situated between 25° and 35° north latitudes (e.g., Gaetani *et al.,* 2000). Such a location resulted in hot and dry to semi-dry climatic conditions, which caused intensified evaporation (Szulc, 2000). Relatively humid climatic conditions prevailed only in the Early and the Late Triassic period, what was evidenced by an input of siliciclastics (Michalík, 1993).

During the Early Triassic, after an episode of alluvial sedimentation (Mišík and Jablonský, 2000), along with peneplanation and a prograded marine transgression, the sedimentary environment changed into estuaries and lagoons and later into a lagoon-sabkha transitional environment (Dżułyński and Gradziński, 1960; Leszczyński and Pszonka, 2014; Rychliński and Jaglarz, 2017). The Middle Triassic is characterized by carbonate sedimentation on a restricted carbonate ramp with episodic storm sedimentation (Jaglarz and Szulc, 2003; Jaglarz and Uchman, 2010). Eustatic sea-level-controlled 3rd-order cycles (Jaglarz and Szulc, 2003) might have been modified by tectonic activity that is indicated by seismites, reported from the Anisian succession in the Tatricum domain (Rychliński and Jaglarz, 2017). At the end of the Ladinian, the area discussed had emerged and during the Carnian–Norian times red-beds-type, fluvial siliciclastics and lagoonal dolostones were deposited (Kotański, 1959b; Al-Juboury and Ďurovič, 1996; Jaglarz, 2010).

The Triassic succession of the Tatricum begins with quartz conglomerates and sandstones, passing upward into mudstones with intercalations of sandstones and dolostones (Roniewicz, 1966). These sediments (with a maximum thickness of 165 m) represent the ?Induanian–lower Olenekian interval (Fuglewicz, 1979; Leszczyński and Pszonka, 2014). The lower part of the upper Olenekian succession consists of dolostones, interbedded with variegated mudstones and cavernous dolostones (about 50 m thick), while its upper part (the so-called Myophoria Beds, about 65 m thick) is composed of dolostones, dolostone breccias, black clayey limestones and black, green and red mudstones (Kotański, 1956, 1959b). The overlying Anisian and Ladinian succession is composed of interbedded limestones and dolostones, which are about 600 m thick.

The biostratigraphic resolution of the late Olenekian–Ladinian succession in the High-Tatric unit is rather poor. Relatively rare index fossils (crinoids, calcareous algae, benthic foraminifers) are restricted to the Anisian interval (see Rychliński *et al.*, 2013). Therefore, the chronostratigraphic assignment of the Olenekian–Ladinian succession is based on sequence stratigraphic considerations (Jaglarz and Szulc, 2003).

As a result of the Early Jurassic tectonic block movements, a complete profile of the succession is preserved in only part of High-Tatric autochthonous unit. Owing to intensive erosion on the horsts, the Middle or even Upper Jurassic deposits cover directly the lower Ladinian and the lower Anisian sediments in the Czerwone Wierchy and the Giewont nappes, respectively (Kotański, 1961; Łuczyński, 2002).

Facies characteristics

Upper Olenekian (Myophoria Beds)

The dolostones are dominated by dolomudstones, often comprising rhomboidal, nodular or nodular-spherolitic pseudomorphs after sulphates (Jaglarz and Rychliński, 2010) with subordinate microbial dolostones (stromatolites), containing enterolithic structures and parallel- or cross-laminated peloidal, bio- and intraclastic dolostones. The latest of these are interpreted as a storm deposits (Jaglarz, 2012). Parallel-laminated, black, clayey limestones (recrystallized to sparite) contain calcite pseudomorphs after sulphates in some places. The lamination resulted from microbial activity or the accumulation of siliciclastic components.

The mudstone layers represent the sediments of episodic floods or have an aeolian origin (Jaglarz and Hryniewicz, 2014). The Myophoria Beds were deposited in a supra- to intertidal sedimentary environment. Repeated emersion episodes are documented by tepee structures, regoliths and synsedimentary karst horizons.

Anisian–Ladinian

The deepest facies are composed of packages of dark-grey calcilutites (massive, bioturbated or banded) with intercalations of thin calcarenite beds (commonly comprising crinoids). Calcilutites and thin calcarenites represent the background sediments and storm deposits, respectively, deposited below normal or storm wave-base (Jaglarz and Uchman, 2010). Shallower facies are represented by oolitic, peloidal and bioclastic calcarenites, several metres thick (largely dolomitized; Jaglarz, 2012), deposited on isolated,

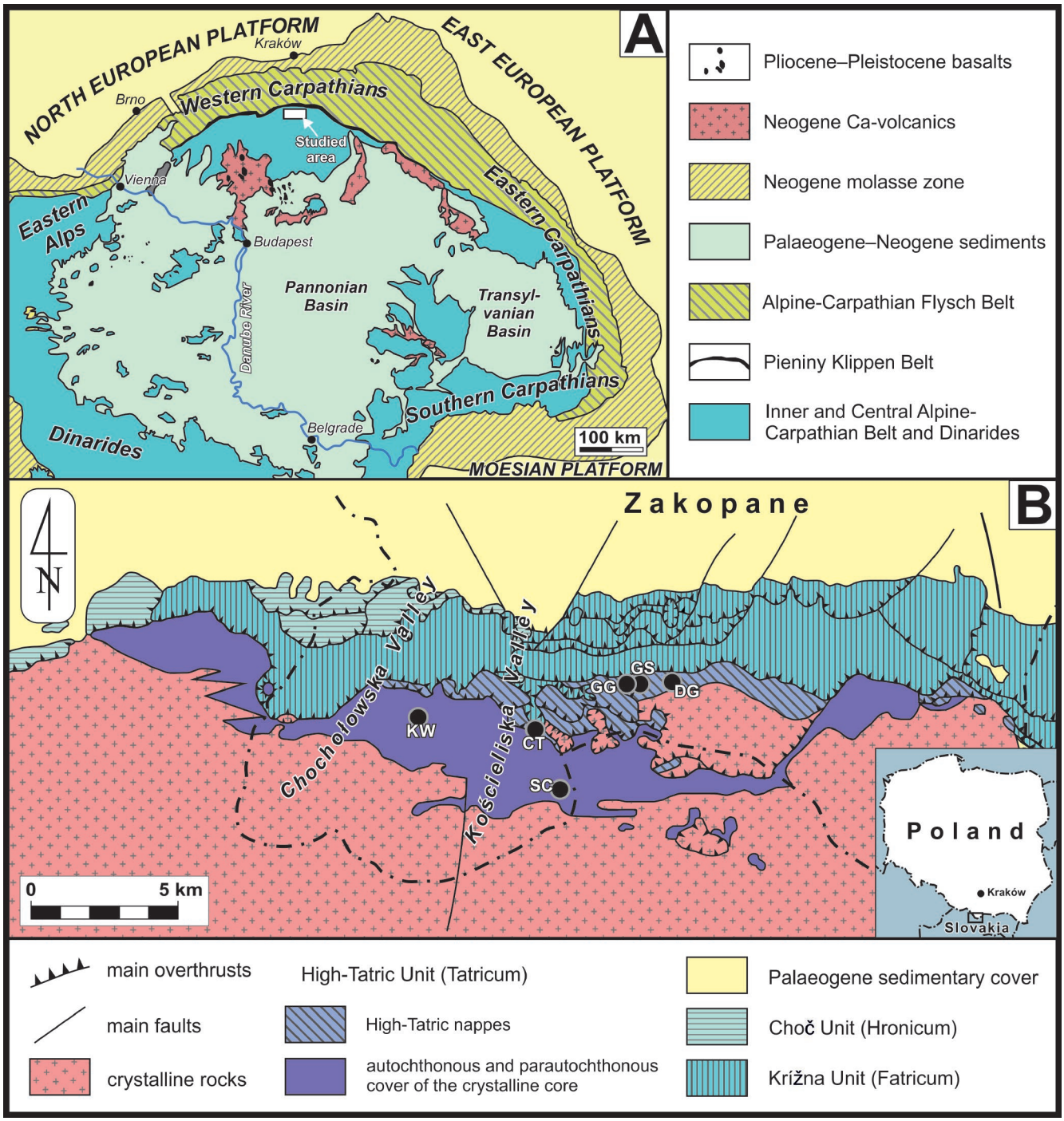

Fig. 1. The study area. **A.** Location of the Tatra Mountains on the geological sketch-map of the Alpine–Carpathian–Pannonian orogenic belt (after Jurewicz, 2005; modified). **B.** Location of the studied sections on the tectonic sketch map of the Tatra Mountains (after Bac-Moszaszwili *et al*., 1979; modified): KW – southern slopes of Kominiarski Wierch Mount, SC – Stoły pod Ciemniakiem (both from the High-Tatric autochthon), CT – pod Chudą Turnią gully above Dolinka Kamienne Zadnie Valley (the Czerwone Wierchy Nappe), GG and GS – southern slopes of Giewont mount and DG – southern slopes of Długi Giewont Ridge (all from the Giewont Nappe).

high-energy, submarine shoals (Jaglarz and Uchman, 2010). The shallowest facies are represented by platy dolostones, dominated by micrite and microsparite dolostones, commonly containing pseudomorphs after sulphates. Stromatolites and microbial dolostones with fenestral structures are also recognized. Elongation of the fenestrae parallel to the stratification indicates their formation, due to desiccation of microbial mats during emersion episodes (Shinn, 1968). Intramicrite dolostones were formed by the erosive destruction of previously cracked microbial mats. The platy dolostones were formed in the supra- to intertidal zone (Jaglarz, 2012). Emersion episodes (less common than in the case of the Myophoria Beds) are documented by teepee and karst horizons (Jaglarz and Szulc, 2003).

MATERIALS AND METHODS

The breccias studied were found in the upper Olenekian and Middle Triassic deposits of the High-Tatric Unit, which were investigated bed-by-bed in six sections (Figs 1B, 2): the Pod Chudą Turnią Gully above Kamienne Zadnie Valley – CT (E19°53′32″, N49°14′12″), the southern slopes of Długi Giewont Ridge – DG (E19°56′20″, N49°14′59″), the southern slopes of Giewont Mount – GS (E19°56′02″, N49°14′56″) and GG (E19°56′00″, N49°14′59″), the southern slopes of Kominiarski Wierch Mount – KW (E19°50′11″, N49°14′05″) and Stoły pod Ciemniakiem – SC (E19°54′18″, N49°13′29″). However, the field observations of breccia features were hampered by vegetation, advanced rock diagenesis and similarity to the under- and overlying dolostones. Therefore, many breccia characteristics were deduced from hand specimens (38) and thin sections (41). All thin sections were stained with an alizarin red S and potassium ferricyanide mixture (Adams *et al.*, 1984). The classification of the breccias is based on the scheme proposed by Morrow (1982). The classification of dolomite textures (Sibley and Gregg, 1987) was adapted to the description of dolomitized breccia matrix (matrix dolomite), dolomite cements (passively precipitated, space-filling crystals, which grow attached to a free surface; Bathurst, 1975) and void-filling dolomites (sensu Sibley and Gregg, 1987). The void-filling dolomites were distinguished in the case of dolomite replacing an earlier cement or when it was impossible to distinguish dolomite cement from dolomite that replaced an earlier-existing matrix or cement.

Cathodoluminescence (CL) petrography was performed, using a Technosyn Model 8200 Mark III cold-cathode instrument (Technosyn Limited, Cambridge, UK), mounted on a binocular petrographic microscope (Nikon Eclipse 50i), equipped with 4x and 10x·objectives and a trinocular photohead with 10x oculars. Such a setup allowed both real-time visual examination and analogue photomicrography, at magnifications of 40 to 100. Operating voltages were held at 13.5 to 15.5 kV and gun current levels at 350 to 450 μA. CL observations were applied to distinguish generations of the different types of dolomite.

RESULTS

Field and macro-scale observations

The breccias studied are sandwiched between undeformed carbonate rocks. The thickness of breccia beds changes in a wide range from 0.5 cm to 6 m. The breccias are characterized by a sharp and flat base (Fig. 3G), while toward the top they gradually pass into undeformed dolostones. The breccias (light to dark grey or reddish) are composed of poorly sorted dolostone clasts (0.2–60 mm across), which represent the same facies as the host dolostones. Angular to sub-angular clasts predominate in the grain framework, although sub-rounded clasts are also present in places (Figs 3F, 4D). The breccias are matrix- or grain-supported (Figs 3A, C–F, 4A–D). The lower parts of breccia bodies are matrix-dominated, where clasts are mostly chaotically arranged, relatively more rounded and represent different facies of dolostones. In contrast, toward the top, the clasts are associated with dolomitic cements, they are more angular with only slight rotation, and generally represent one type of facies (Fig. 3A, B, E). Inverse grading is rare (Fig. 3A, E). In the cases, where the intergranular pores are filled with both matrix and cements, the matrix fills only their basal part, forming geopetal structures (Fig. 3C). In some places, the matrix is reddened by iron hydroxides/oxides (Fig. 3B, D, H).

According to the classification by Morrow (1982), the rocks discussed range from monomictic, cemented mosaic packbreccias to chaotic, unsorted, oligomictic, particulate/cemented rubble floatbreccias.

Micro-scale features

The breccia clasts are dominated by dolomicrites and dolomicrosparites, which commonly contain nodular pseudomorphs after sulphates (Fig. 4A–C). Fine-crystalline dolosparites, dolopelsparites, dolopelmicrites as well as dolobiosparites, containing ostracods and microbialites, are subordinate and claystones occur only in places in some breccia horizons (Fig. 4D). The boundaries between the clasts of the breccia framework and the matrix are sharp, except for some dolosparite clasts.

The matrix is composed of micrite, in places with an admixture of clay minerals and/or quartz silt (Fig. 5E, G). The micrite is partially or completely dolomitized, forming matrix dolomite (the unimodal, nonplanar, replaced matrix dolomite; Figs 5A, 6C; Table 1).

The remaining part of the pore space was filled by different type of dolomite cements and void-filling dolomites, which were distinguished in the basis of the shape of the crystal edges, the crystal size and the degree of crystal size unification (Table 1).

Dolomite cement 1 (polymodal, planar-s dolomite cement) fills voids of intergranular space or vugs after dissolved evaporites in clasts of dolostones (Fig. 5A, G), while dolomite cement 2 (polymodal, planar-e dolomite cement) is restricted only to the margins of such voids (Fig. 6A, C). Void-filling dolomite 1 (the polymodal, nonplanar dolomite nonmimically replaced sulphates) and 3 (polymodal, planar-e void-filling dolomite) replaces sulphate cement in the matrix with an admixture of clays (Figs 4E, 5E–H, 6A). Void-filling dolomite 1 replaces the sulphate cement of breccias at the top of the upper Olenekian succession. Although the evaporite minerals were dissolved, dolomite

Fig. 2. Generalized lithological sections of the upper Olenekian–Ladinian succession from the High-Tatric Unit (Tatricum domain) in the Tatra Mts. From the left: KW, SC, CT, GG, GS and DG sections (explanation of abbreviations in the Fig. 1B). Black arrows indicate horizons of solution-collapse breccias interpreted by Kotański (1954, 1956) as transgressive breccias. Chronostratigraphy based on Jaglarz (2007).

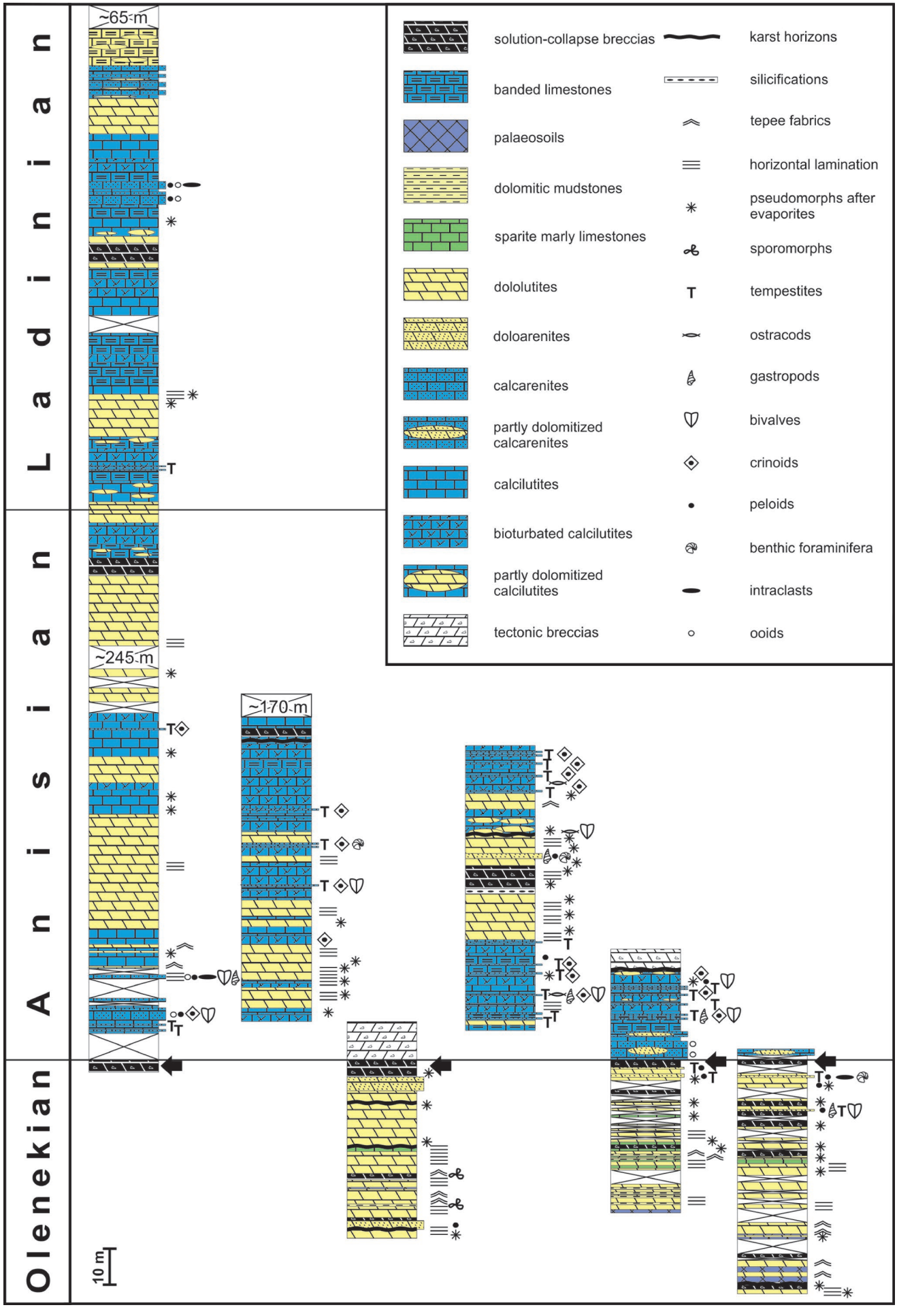
Ladinian
Anisian
Olenekian
~65 m
~245 m
~170 m
10 m
solution-collapse breccias
banded limestones
palaeosoils
dolomitic mudstones
sparite marly limestones
dololutites
doloarenites
calcarenites
partly dolomitized calcarenites
calcilutites
bioturbated calcilutites
partly dolomitized calcilutites
tectonic breccias
karst horizons
silicifications
tepee fabrics
horizontal lamination
pseudomorphs after evaporites
sporomorphs
T tempestites
ostracods
gastropods
bivalves
crinoids
peloids
benthic foraminifera
intraclasts
ooids

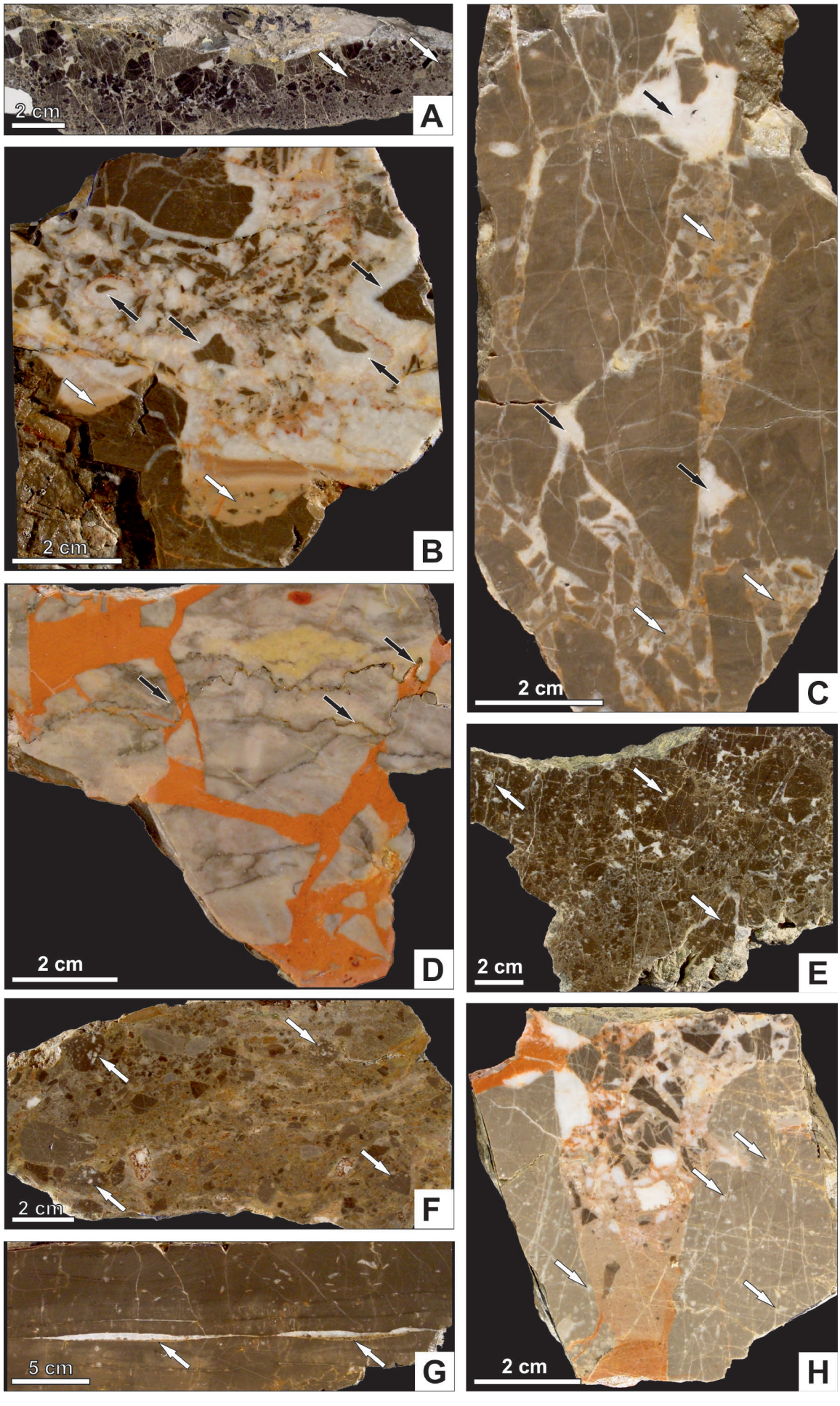
2 cm
A
2 cm
B
2 cm
C
2 cm
D
2 cm
E
2 cm
F
5 cm
G
2 cm
H

pseudomorphs after them mimic the shapes of the primary sulphate crystals. The pseudomorphs comprise small inclusions of clays. Void-filling dolomite 3 in the laminated, reddish matrix of the Anisian breccias of the GS section represents pseudomorphs after gypsum crystals, as indicated by their lozenge shape (see Vogel *et al*., 1990). Void-filling dolomite 2 (the polymodal, nonplanar, void-filling dolomite) replaces micrite in voids of intergranular space or fills vugs in clasts after dissolved evaporites (Fig. 5C). Saddle (baroque) dolomite occurs in the voids of intergranular space and fractures. Commonly, dolostone clasts are supported by saddle dolomite (Fig. 6E, G). In places, the dolomite cements and the saddle dolomite are accompanied by calcite cement, which fills the central parts of intergranular spaces (Fig. 6C, G).

The matrix dolomite and the dolomite cement 1 are the most common among the dolomite types described above, while the others are subordinate. Almost every dolomite type under consideration does not stain with an alizarine red S and potassium ferricyanide mixture. Only some saddle dolomites stain as pale blue.

The breccias described are rich in stylolites (Fig. 4E), which may cut across clasts, matrix and cement. The breccias (clasts, matrix and cements) and both the under- and overlying dolostones are commonly fractured (Fig. 4B, D). The fractures are filled by calcite spar. This calcite spar is identical to the calcite cement, filling the central parts of the intergranular space of the solution-collapse breccias.

CL observations

CL pattern of the dolomite crystals reveals generations of their growth (Table 1). The cores of the matrix dolomite crystals (rarely the entire crystal) are anhedral and display homogeneous or mottled (red to dull red) luminescence (Figs 5A, B, 6C, D). The cores were accreted as successive generations of dolomite in the form of dull, red bands or thin, orange rims (Fig. 5B). Only generation I of the void-filling dolomite 1 (red with thin, orange rim CL pattern) represents pseudomorphs after sulphates that mimic the shapes of the primary crystals, whereas generation II grew directly on them (Figs 5E–H, 6A, B).

Generations I, II and III of dolomite cement 1 and void-filling dolomite 2 display similar CL characteristics within each generation (Fig. 5A–D, G, H). Generation I is characterized by clear, concentric zonation (from nonluminescent to bright, orange bands) and is represented by euhedral crystals. Furthermore, the CL characteristics of dolomite cement 2 correspond to that generation (Fig. 6A–D). Generation II is dull red to nonluminescent, in places with a weak zonation, while generation III is homogeneous, red or orange.

CL observations indicate that saddle dolomite filled intergranular space or partly replaced dolostone clasts of breccia (Fig. 6E–H). Generation I of these crystals is characterized by clear zonation (dull red to orange), while generation II is characterized by indistinct zonation with dull red to nonluminescent bands. Moreover, the latter generation of baroque dolomite is pale blue after staining with an alizarine red S and potassium ferricyanide mixture. Void-filling dolomite 3 displays an orange (generation I) or nonluminescent (generation II) CL pattern. The calcite cement is characterized by dull red or mottled dull red to an absence of luminescence.

INTERPRETATION

Brecciation process

The sharp and flat base of the breccias can be referred to the dissolution of evaporites (Middleton, 1961). The removal of the evaporite beds caused the formation of voids with flat bases, reflecting the primary boundary between the evaporite bed and the underlying dolostones (Simpson, 1988). Although the evaporites are no longer present, the breccia clasts and host dolostone beds contain pseudomorphs after sulphates, which are among the most important indicators of the solution-collapse origin of a breccia (Scholle *et al.*, 1993). The thicknesses of breccia beds (less than 6 m) indicate that the thicknesses of the evaporite beds were relatively small.

The brecciation mechanism was characterized by the gradual dissolution of the evaporite beds and the progressive collapse of the interbedded dolostones, as indicated by the arrangement of overlying beds parallel to general

---

Fig. 3. Structural and textural features of the dolostone solution-collapse breccias (hand specimens). **A.** Oligomictic (composed of different kind of dolostone clasts) breccia with inverse grading. Particulate/cemented rubble floatbreccia in the lower and right part, cemented rubble packbreccia in the upper left part. Clasts with dolomite pseudomorphs after sulphates (white arrows). The breccia is merged by matrix containing clays and dolomite pseudomorphs after sulphate cement. KW section, upper Olenekian. **B.** Chaotic monomictic cemented rubble float-/packbreccia. Reddish insoluble residuum after dissolution of dolostones (white arrows). Breccia cemented by saddle dolomite; clasts are partly replaced by mentioned cement (black arrows). GS section, Anisian. **C.** Unsorted cemented/particulate mosaic packbreccia with geopetal structures; lower part of intergranular pores filled with matrix (white arrows) while their upper part filled with dolomite cement (black arrows). GG section, Anisian. **D.** Monomictic particulate rubble floatbreccia. Breccia is merged by residual dolomitic claystones reddened by iron hydroxides/oxides. Stylolites (black arrows) intersect clasts and matrix. GS section, Anisian. **E.** Chaotic monomictic particulate/cemented rubble float-/packbreccia with inverse grading. Clasts contain pseudomorphs after sulphates (white arrows). DG section, upper Olenekian. **F.** Chaotic unsorted oligomictic particulate/cemented rubble floatbreccia. The breccia is merged by matrix with admixture of clays and dolomite pseudomorphs after sulphate cement. Clasts with dolomite pseudomorphs after sulphates (white arrows). GS section, upper Olenekian. **G.** Microbreccia (white arrows). Clasts in the lower part and dolomite cement in the upper part. Sharp base is visible. Under- and overlying dolostones comprise evaporite pseudomorphs. DG section, upper Olenekian. **H.** Unsorted oligomictic particulate/cemented rubble float-/pack breccias. Matrix contain reddish oxidized iron compounds. Dolomite pseudomorphs after sulphates (white arrows) in clasts. CT section, upper Olenekian.

stratification (Swennen *et al.*, 1990). Where brecciation was caused by the formation of caverns, followed by the collapse of their ceilings, inverse-graded breccias have been formed (Eliassen and Talbot, 2005), but in the breccias described such structures are rare.

The advancing filling of voids reduced space for rotation of clasts. Therefore, in individual breccia beds, the degree of deformation (chaotic arrangement and rotation of clasts, their roundness and microfacies diversification) decreases upward (Eliassen and Talbot, 2005). Consequently, the mosaic breccias occur in the upper parts of the breccia beds (Fig. 3C). The roundness of clasts resulted either from abrasion or from partial dissolution, as postulated (Simpson, 1988). It should be noted that the clasts of breccia discussed do not display ductile deformation. This suggests that sediment collapse was preceded by the complete lithification of the host dolostones (cf. Karakitsios and Pomoni-Papaioannou, 1998).

The origin of the matrix might be linked to gravitational infiltration of the uppermost, unconsolidated, fine-grained

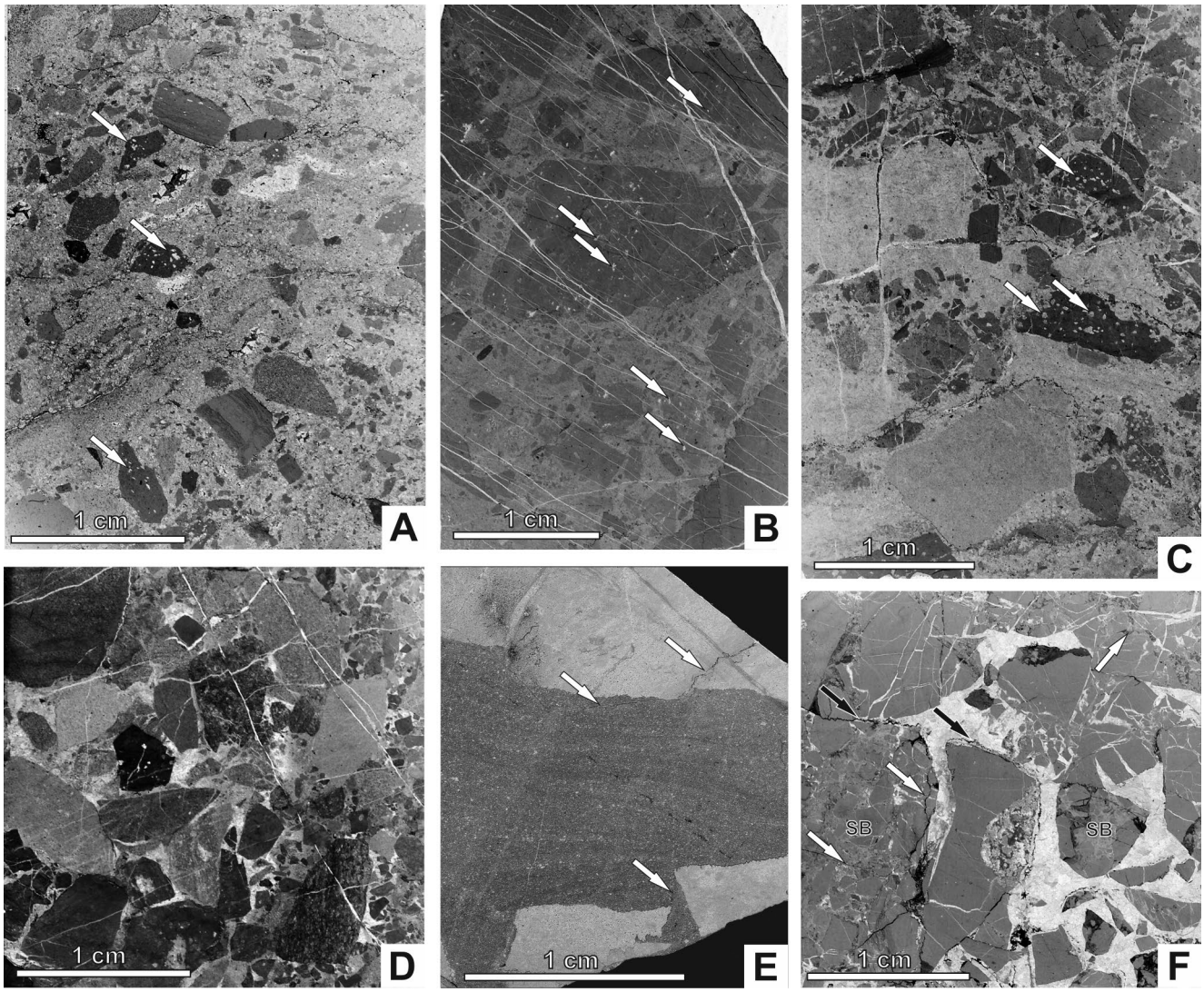

Fig. 4. Structural and textural features of the dolostone solution-collapse breccias (scanned thin sections). **A.** Chaotic unsorted oligomictic particulate/cemented rubble floatbreccia. Clasts from angular to subrounded. The breccia is merged by matrix containing clays and dolomite pseudomorphs after sulphate cement. Clasts with dolomite pseudomorphs after sulphates (white arrows). GS section, upper Olenekian. **B.** Chaotic unsorted monomictic particulate rubble floatbreccia. Clasts include dolomite pseudomorphs after sulphates (white arrows). Matrix is composed of dolomitized micrite. Clasts and matrix are fractured (fractures filled with the calcite cement). SC section, Anisian. **C.** Chaotic unsorted oligomictic particulate/cemented rubble pack-/floatbreccia. The breccia is merged by matrix with admixture of clays and dolomite pseudomorphs after sulphate cement. Clasts with dolomite pseudomorphs after sulphates (white arrows). CT section, upper Olenekian. **D.** Chaotic unsorted oligomictic cemented rubble packbreccia. Clasts and matrix are fractured (fractures filled with calcite cement). KW section, upper Olenekian. **E.** Monomictic particulate rubble floatbreccia. Residual sediment consists of dolomitized micrite with admixture of clay minerals, dispersed reddish oxidized iron compounds and lozenge dolomite crystals (pseudomorphs after gypsum) arranged in laminae. Stylolites (white arrows) intersect clasts and matrix. GS section, Anisian. **F.** Tectonic breccia composing of dolostone and solution-collapse breccia clasts (SB) cemented by calcite spar. Stylolites fit to clasts edges (black arrows) or intersect clasts only (white arrows). Clasts of solution-collapse breccia are distinguished, owing to the presence of the dolomite cements.

Table 1

Petrography, staining and CL pattern of dolomites and calcite cement in the solution-collapse breccia bodies of the upper Olenekian–Ladinian succession of the High-Tatric Unit in the Tatra Mts

Dolomite type	Matrix dolomite	Void-filling dolomite 1	Void-filling dolomite 2	Void-filling dolomite 3	Dolomite cement 1	Dolomite cement 2	Saddle (baroque) dolomite	Calcite cement
Occurrence	carbonate matrix of breccias	area primarily occupied by sulphate crystals	voids and vugs (partly after dissolved evaporites)	places primarily occupied by gypsum crystals	voids, vugs (partly after dissolved evaporites)	voids margins	voids, vugs or fractures	vugs or fractures
Crystal size	unimodal, finely to medium crystalline (0.03–0.18 mm)	polymodal, coarsely crystalline (0.28–0.61 x x 0.12–0.34 mm)	polymodal, medium- to coarsely crystalline (0.11–0.45 mm)	polymodal, finely to medium crystalline (0.04–0.17 mm)	polymodal, medium- to coarsely crystalline (0.13–1.00 mm)	polymodal, medium- to coarsely crystalline (0.11–0.66 mm)	polymodal, coarsely to very coarsely crystalline (0.85–2.71 mm)	medium to very coarsely crystalline (0.21–4.6 mm)
Crystal shape	anhedral	anhedral, bar or isometric shape	anhedral to subhedral	euhedral	subhedral to anhedral	euhedral to subhedral	anhedral (saddle dolomite)	anhedral
Fabrics	unimodal nonplanar (partially) replaced matrix dolomite	polymodal nonplanar dolomite nonmimically replaced sulphates	blocky or drusy mosaics of polymodal non-planar void-filling dolomite	polymodal planar-e void-filling dolomite	blocky or drusy polymodal planar-s dolomite cement	drusy polymodal planar-e dolomite cement	polymodal non-planar (saddle) dolomite cement	mosaic
Extinction	straight	straight	straight	undulose	partly undulose	undulose	sweeping	straight
Staining	unstained	unstained	unstained	unstained	unstained	unstained	unstained (I generation); unstained or pale blue (II generation)	red
CL pattern	two generations: homogeneous or mottled dull red to red (I); commonly with dull red band and/or thin orange rim (II)	two generations: red with thin orange rim (I), dull red sometimes with weak concentric zonation or nonluminescent (II)	three generations: nonluminescent through orange, to red; concentric zonation (I), dull red to nonluminescent with thin bright red rims; weak concentric zonation (II), red (III)	two generations: orange (I) or nonluminescent (II); sometimes orange in central part of the crystals	three generations: dull red to bright orange; concentric zonation (I), dull red or nonluminescent (II), orange (III)	nonluminescent to orange; concentric zonation	two generations: dull red to orange; concentric zonation; central part of crystals dull red or mottled dull red and red (I), dull red or dull red to nonluminescent (weak concentric zonation; II)	dull red or mottled dull red to nonluminescent
Other crystals features	–	pseudomorphs after sulphate crystals; cross-type twins (generation I)	cloudy (orange to red zones in the generation I)	–	cloudy in the core (generation I), core of crystals euhedral in shape	partly cloudy	cloudy; corrosion of the crystals on contact with calcite cements	partly cloudy

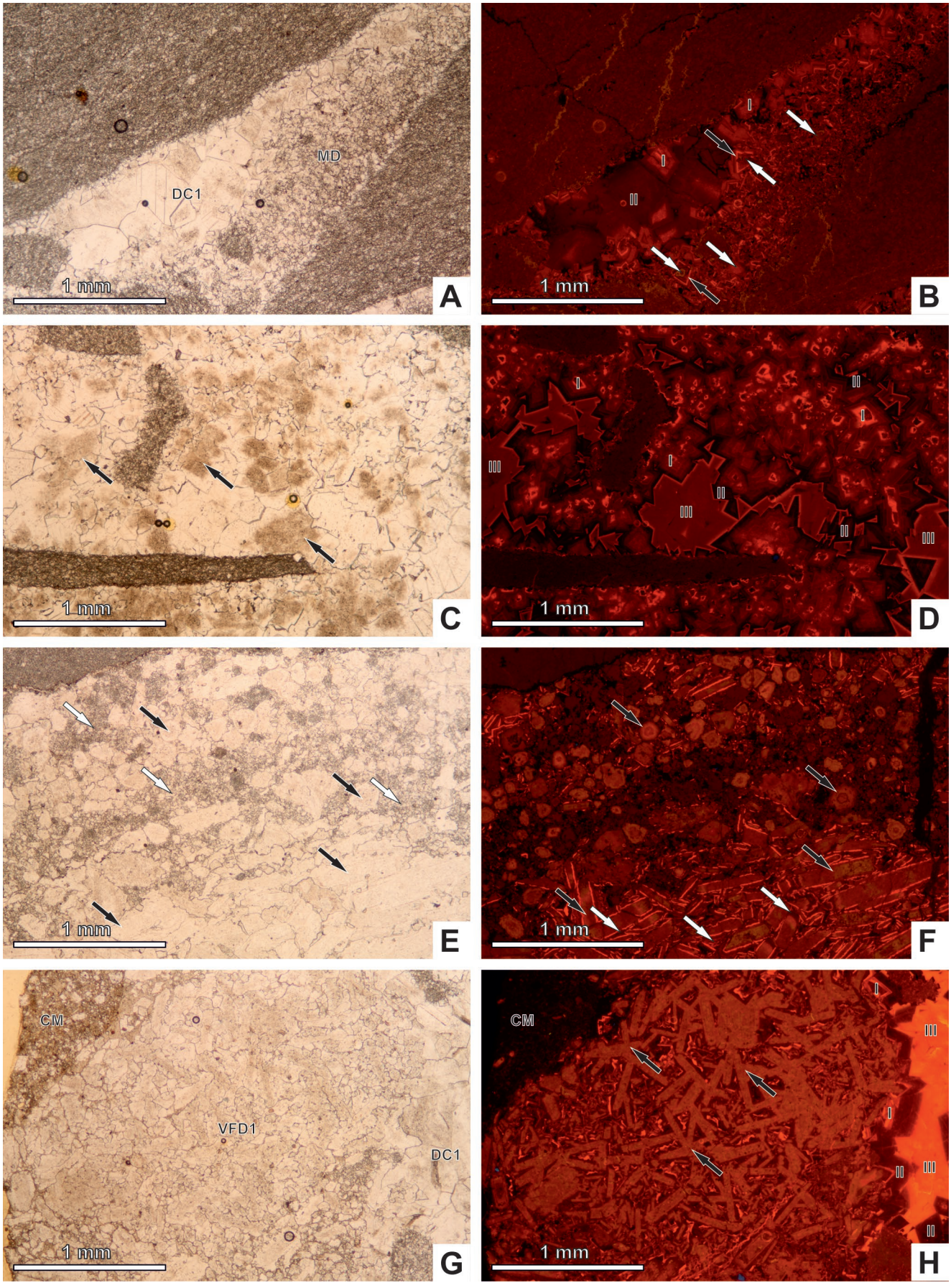
MD
DC1
1 mm
A
I
II
1 mm
B
1 mm
C
III
1 mm
D
1 mm
E
1 mm
F
CM
VFD1
DC1
1 mm
G
CM
1 mm
H

sediments (see Swennen *et al.*, 1990). During the gradual brecciation or soon after it, the cavities at the basal parts of the breccia bodies were partially or completely filled by these fines.

The reddish matrix, consisting of iron hydroxides/oxides (Figs 3B, D, H, 4E), is probably the insoluble residuum after the intensive leaching of evaporites and/or carbonates (cf. Scholle *et al.*, 1993; Pomoni-Papaioannou and Karakitsios, 2002). It indicates that in places the evaporite/carbonate sequences were subjected to karstification. Additionally, the presence of lozenge pseudomorphs after gypsum confirms that this kind of matrix is an equivalent of the solution-formed residues derived from within the evaporite sequences (see Simpson, 1988). Redeposition of the reddish matrix is evidenced by the lamination, defined by the lozenge pseudomorphs after gypsum (Fig. 4E).

The breccia features described above indicate that their origin was linked with the collapse of dolostone layers, preceded by the dissolution of evaporites.

Diagenesis of the breccias

Sulphate cementation

The brecciation was followed by cementation of the breccias at the top of the upper Olenekian succession by sulphate minerals (Figs 2, 3A, F, 4A, C). The well-preserved shape of the pseudomorphs after sulphates indicates that the evaporites were precipitated after brecciation (Figs 5E–H, 6A, B). Otherwise, the collapse of the sediments would lead to crystal crushing. Moreover, the inclusions of fine clays indicate that the evaporite crystals grew in a non-lithified matrix. A similar process was observed in halite crystals growing in siltstones (Rychliński *et al.*, 2014).

Dolomitization

Significant aspects of the diagenesis of the breccias are the dolomitization of the matrix and their cementation by dolomite.

The paragenetic relationships between the different types of dolomite and a correlation of particular crystal generations from the different dolomite types indicate that the sequence of events in the breccias was as shown in Table 2. First, the breccia matrix was replaced by dolomite (generation I of the matrix dolomite). Sulphate cements were dissolved after the lithification of the matrix dolomite. Otherwise, the voids after sulphates could not be preserved so perfectly. Thus, generation I of void-filling dolomite 1 was formed after generation I of the matrix dolomite (Fig. 5E–H). These processes preceded the precipitation of generation I of dolomite cement 1 and void-filling dolomite 2 as well as dolomite cement 2 (Figs 5A–D, 6A–D). In addition, the matrix dolomite accreted during this stage of dolomitization. Void-filling dolomite 1 accreted, and generations II and III of both dolomite cement 1 and void-filling dolomite 2 were precipitated during two subsequent stages of dolomitization (Table 2). The saddle dolomite and void-filling dolomite 3 (pseudomorphs after gypsum) were formed last.

The range of crystal sizes and the shapes of crystal edges depended on a number of factors, such as the temperature of the fluids and their saturation with respect to dolomite, the conditions of nucleation, the rate of crystal growth and finally the mineralogy of the dolomitized material (Sibley and Gregg, 1987).

Main factor controlling the intensity of CL in dolomite crystals is the Mn/Fe ratio (Miller, 1988). The concentration level of both Mn^{2+} and Fe^{2+} is higher in carbonates precipitated in more reducing conditions (Boggs and Krinsley, 2006). The lack of staining (except generation II of saddle dolomite) indicates that the dolomites are not ferruginous and indicates that the intensity of CL in the samples studied depends mostly on changes in the Mn^{2+} content (Miller, 1988).

The characteristics of dolomite crystals mainly depend on the chemical composition of the dolomitizing fluids (Ren and Jones, 2018). The nonplanar crystal boundary shape of generation I of the matrix dolomite indicates that the dolomitization process might have occurred under the influence of fluids, supersaturated with respect to dolomite (Gregg and Sibley, 1984; Sibley and Gregg, 1987). Additionally, the fine size of the crystals and their cathodoluminescence features indicate a relatively early diagenetic origin of the dolomite (Amthor and Friedman, 1991). It follows that this phase of dolomitization took place in near-surface conditions under the influence of hypersaline solutions. Generation I of the matrix dolomite represents the first stage of the solution-collapse breccias dolomitization.

The second stage of dolomitization of the breccias studied is represented by generation I of the void-filling dolomite 1 (Table 2). Generation I of dolomite cement 1 and

Fig. 5. Diagenetic features of the solution-collapse breccias; thin sections stained with alizarin red S + potassium ferricyanide solution (view in transmitted light on the left and under cathodoluminescence on the right). **A.** The matrix dolomite (MD) and dolomite cement 1 (DC1) filling intergranular pore space. DG section, upper Olenekian. **B.** Crystals of the matrix dolomite with homogenous or mottled core (generation I; white arrows) commonly banded by generation II (black arrows) analogous to generation I of dolomite cement 1; two generations of dolomite cement 1 (I, II). **C.** The intergranular pore space occupied by void-filling dolomite 2 replacing earlier micrite matrix which relicts are preserved in places (arrows). DG section, upper Olenekian. **D.** Generations I and II of void-filling dolomite 2 – the effect of micrite replacing by dolomite spar; generation III of void-filling dolomite 2 fills the pore space. **E.** Void-filling dolomite 1 (black arrows) in matrix with admixture of clays (white arrows). CT section, upper Olenekian. **F.** Void-filling dolomite 1 compose of orange rimmed dolomite pseudomorphs after sulphate crystals (generation I of void-filling dolomite 1; black arrows) is accreted by generation II of void-filling dolomite 1 (white arrows). **G.** Matrix with admixture of clay minerals (CM), void-filling dolomite 1 (VFD1) and dolomite cement 1 (DC1). KW section, upper Olenekian. **H.** Matrix with admixture of clay minerals (CM), void-filling dolomite 1 (central part) – dolomite pseudomorphs after sulphate crystals with cross-type twins (black arrows), generations I, II and III of dolomite cement 1.

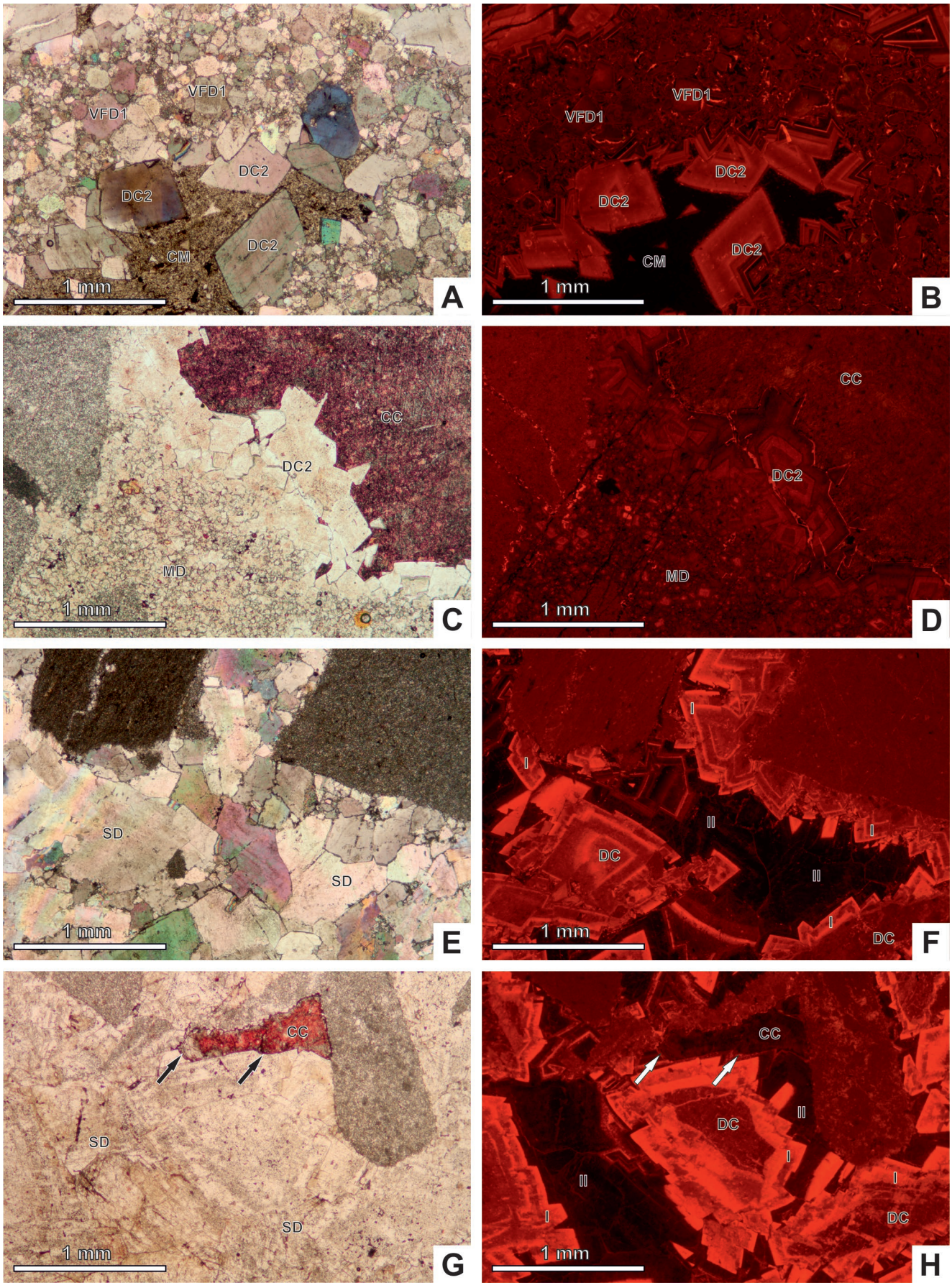
VFD1
VFD1
DC2
DC2
DC2
CM
1 mm
A
VFD1
VFD1
DC2
DC2
CM
DC2
1 mm
B
CC
DC2
MD
1 mm
C
CC
DC2
MD
1 mm
D
SD
SD
1 mm
E
I
I
II
I
DC
II
I
1 mm
DC
F
CC
SD
SD
1 mm
G
CC
DC
II
I
II
I
I
DC
1 mm
H

void-filling dolomite 2 as well as dolomite cement 2 represent the third stage of dolomitization. Their idiotopic texture indicates low saturation of the solutions with respect to dolomite (Sibley and Gregg, 1987). Under the CL, crystals of the last-mentioned dolomite types are characterized by zonation with a predominance of red and orange colours. It indicates that they were formed during burial under reducing conditions (Boggs and Krinsley, 2006). However, the crystal zonation does not have to be related to fluctuations of Eh during crystallization. The changes in the concentration of Mn^{2+} in crystals are also caused by other factors, such as changes in the Mn^{2+} content of the dolomitized fluids or fluctuations in the rate of crystal growth; the faster the crystal growth, the more Mn^{2+} ions are incorporated (Miller, 1988). The idiotopic texture of the dolomite crystals indicates their slow growth (Sibley and Gregg, 1987). Thus, crystal zonation is related to the first of these factors.

Generation II of both dolomite cement 1 and void-filling dolomite 2 (nonluminescent) represents a fourth stage of breccia dolomitization, which took place in oxidizing conditions. Such conditions might have been connected with the influx of oxygenated fluids during the repeating periods of sea-level lowstand. Generation III of both dolomite cements 1 and void-filling dolomite 2 represents a fifth stage of dolomitization (Fig. 5C, D, G, H). This generation of dolomites was formed in reducing condition during deeper burial, as indicated by uniform red or orange luminescence (Tables 1, 2).

The saddle (baroque) dolomites are among others associated with calcite and are common in carbonates that are rich in sulphates (Radke and Mathis, 1980). Generally, saddle dolomites are considered to have been formed as a result of dolomitization in temperatures of above ca. 60–80 ºC (e.g., Spötl and Pitman, 1998). They might have been formed in different ways, including in intermediate to deep burial settings (Machel, 2004). Nevertheless, they crystallized from solutions, characterized by high salinities (e.g., Amthor and Friedman, 1991).

Among the dolomite types discussed, only generation II of saddle dolomite (the seventh stage of dolomitization) is ferruginous (pale blue colour after staining; Adams and MacKenzie, 1998). Dull red luminescence or nonluminescence indicate Fe^{2+} as a quencher (Machel, 2000).

DISCUSSION

Most of the breccias described were identified by Kotański (1954) as intraformational and interpreted as subaquatic deposits that had resulted from the erosion and crushing of previously cemented carbonate sediments because of a deepening of the wave-base. Breccias at the top of the upper Olenekian succession were interpreted as transgressive breccias (Kotański, 1954, 1956). Such an interpretation resulted from the presence of clasts with pseudomorphs after evaporites and clasts of green mud-shales, supposedly derived from the older Lower Triassic rocks, occurring 15 and 40 m below the breccia base (Kotański, 1954). However, dolostones with pseudomorphs after evaporites and layers of green mud-shales are repeated in the upper Olenekian succession (Kotański, 1959a; Jaglarz, 2012). Thus, their presence in the breccia framework does not have to indicate the erosion of older rocks and does not exclude other brecciation mechanisms.

Jurewicz (2005) suggested a hydro-tectonic genesis for the breccias, but did not exclude the possibility that some of them represent sedimentary breccias, modified during later tectonic processes. Primary and diagenetic features of the solution-collapse breccias studied exclude a hydro-tectonic origin, although tectonic breccias are common in the entire upper Olenekian–Middle Triassic succession. The breccias discussed were only modified by the tectonic processes mentioned, which resulted in the development of fractures filled with the calcite spar. In places, the development of the system of fractures led to the rebrecciation of the solution-collapse breccias and clasts of them were incorporated to the tectonic breccias (Fig. 4F). In addition, the stylolites in the breccias of tectonic origin are fitted to the clasts or only cut the clasts. This indicates that such breccias were formed during or after chemical compaction. Fracturing and re-brecciation could be linked with hydro-tectonic phenomena, resulting from changes in pore fluid pressure, which led to hydraulic fracturing and pressure dissolution during overthrusting movements (Jurewicz, 2003, 2005; Jurewicz and Słaby, 2004).

Juxtaposition of structural and textural features of the breccias studied with the features of solution-collapse breccias, known from other research, clearly indicates that the

---

Fig. 6. Microscale diagenetic features of the solution-collapse breccias (view in transmitted light on the left and under cathodoluminescence on the right); thin sections stained with alizarin red S + potassium ferricyanide solution. **A.** Void-filling dolomite 1 (VFD1). Dolomite cement 2 (DC2) rimming void in solution-collapse breccia (filled earlier by matrix with admixture of clays; CM); dolomite cement 2 grew in matrix; crossed nicols. GS section, upper Olenekian. **B.** Matrix with admixture of clay minerals (CM), dolomite cement 2 (DC2) – nonluminescent to orange crystals with concentric zonation, void-filling dolomite 1 (pseudomorphs after sulphate crystals; VFD1). **C.** Matrix dolomite (MD) replacing micrite matrix; dolomite cement 2 (DC2) rimming void in solution-collapse breccia, central part of the void (stained red) filled with the calcite cement (CC). CT section, upper Olenekian. **D.** Matrix dolomite (MD); dolomite cement 2 (DC2) – dull red to red crystals with concentric zonation; the calcite cement (CC). **E.** Breccia merged by saddle dolomite (SD) with sweeping extinction; crossed nicols. GS section, Anisian. **F.** Two generations of saddle dolomite; generation I with red to orange growth bands (overgrowing dolostone clasts) and weakly zoned generation II with indistinct dull red to nonluminescent zones. Relicts of dolostone clasts (DC). **G.** Breccia merged by the saddle dolomite (SD); corrosive boundary between calcite cement (CC) and saddle dolomite (black arrows). GS section, Anisian. **H.** Generations I and II of saddle dolomite; corrosive boundary between calcite cement (CC) and saddle dolomite (white arrows). Relicts of dolostone clasts (DC).

Table 2

Stages and environments of dolomitization of the solution-collapse breccias in the upper Olenekian–Ladinian succession of the High-Tatric Unit in the Tatra Mts. Individual stages are represented by generations of the different types of dolomite. The individual stages or their groups represent the particular diagenetic environments of dolomitization

Dolomitization stages of the breccias	Effect of particular dolomitization stages				Diagenetic environment
stage 1	generation I of matrix dolomite				**near-surface**
stage 2	generation I of void-filling dolomite 1				**shallow burial**
stage 3	generation II of matrix dolomite	generation I of dolomite cement 1	generation I of void-filling dolomite 2	dolomite cement 2	
stage 4	generation II of void-filling dolomite 1	generation II of dolomite cement 1	generation II of void-filling dolomite 2		
stage 5	generation III of dolomite cement 1	generation III of void-filling dolomite 2			**intermediate to deep burial**
stage 6	generation I of void-filling dolomite 3	generation I of saddle dolomite			
stage 7	generation II of void-filling dolomite 3	generation II of saddle dolomite			

rocks studied are of solution-collapse origin (see Middleton, 1961; Simpson, 1988; Swennen *et al.*, 1990; Friedman, 1997; Pomoni-Papaioannou and Karakitsios, 2002; Eliassen and Talbot, 2005).

The reconstruction of relative time and conditions of breccia formation requires determination of the sequence of pre- and post-formation processes. Solution-collapse breccias might be formed during different stages of sediment diagenesis, usually as a result of multi-stage processes (e.g., Pomoni-Papaioannou and Karakitsios, 2002). Solution-collapse breccias could form on the relatively early stage of diagenesis, during the repeated emersion of peritidal deposits (e.g., Vogel *et al.*, 1990; Friedman, 1997; Karakitsios and Pomoni-Papaioannou, 1998), during post-sedimentary emersion of formations containing evaporites (e.g., Swennen *et al.*, 1990; Pomoni-Papaioannou and Carotsieris, 1993; Scholle *et al.*, 1993; Eliassen and Talbot, 2005) or during post-orogenic uplift of a rock complex and the intense leaching of evaporites by ground-water (telogenetic alteration; e.g., Pomoni-Papaioannou and Karakitsios, 2002).

Undoubtedly, the formation of breccias discussed was preceded by the formation of the host dolostones, which were probably interbedded with sulphates before their dissolution. Pseudomorphs after evaporites, sparse ichnofossils and body fossils together with geochemical data indicate the predominance of hypersaline conditions in the sedimentary basin during late Olenekian–Middle Triassic time (Jaglarz and Szulc, 2003; Jaglarz and Uchman, 2010). The host dolostones were formed in the supra- and intertidal zone during early diagenetic dolomitization of lime muds under the influence of hypersaline waters. Such an origin of the host dolostones is evidenced by the preservation of sedimentary structures, the fine-grained fraction (except for redeposited deposits), the relatively high concentration of siliciclastics, pseudomorphs after sulphates, the lack of benthic fauna (except in storm deposits) and teepee structures as well as the pattern of changes of $\delta^{13}C$ values (Jaglarz, 2012). The relation of solution-collapse breccias with hypersaline, shallow-marine sediments is a common phenomenon (Vogel *et al.*, 1990; Friedman, 1997).

A separate problem is determining the timing of diagenetic processes, which occurred after the dissolution of evaporites and subsequent sediment collapse. Undoubtedly, sulphate cementation of the breccias as well as matrix dolomitization and the formation of the dolomite cements postdate the collapse processes. The evaporites were removed

before the infilling of pores by dolomite spar. This is confirmed by the lack of evaporite inclusions in the dolomite crystals, which fill the voids resulting from sulphate dissolution (Scholle *et al.,* 1993). Furthermore, both stylolite formation and hydro-tectonic processes postdate dolomitization of the solution-collapse breccias because stylolites as well calcite veins transect clasts, matrix and cement.

As shown above, the formation of the dolomites postdating the brecciation was a multi-stage process. However, the lack of late diagenetic dolomites in the rocks younger than Middle Triassic indicates that this process had finished before the Late Triassic (Jaglarz, 2012). However, Veizer (1970) indicating that dolomitization processes could have taken place even later, but the red beds of the Upper Triassic and the detrital sediments of the Lower Jurassic hampered the upward migration of dolomitized fluids. If so, processes of dolomitization should have been finished before the Middle Jurassic, since the Middle Jurassic carbonates, covering directly Middle Triassic (e.g., in the Giewont Nappe), do not show any sign of dolomitization. The formation of the dolomite cements was preceded by dolomitization of breccia matrix. Probably, such process occurred under the influence of solutions supersaturated with respect to dolomite and/or in temperatures exceeding 50 ºC (Sibley and Gregg, 1987). Both sets of conditions are met in a sabkha environment, where such temperatures are reached at just over a dozen centimetres below the sediment surface (Gregg and Sibley, 1984). Thus, considering the sedimentary environment of the deposits hosting the breccias studied, it can be assumed that dolomitization of the breccia matrix started under near-surface conditions. It seems that the earliest process that took place after the formation of the solution-collapse breccias was their cementation by sulphate minerals, what is a common phenomenon (Friedman, 1997). Their precipitation took place near the surface from solutions, saturated with respect to sulphates.

If it is proved that the breccias formed at a relatively early stage of diagenesis, the question remains as to what conditions could have occurred. Hot and arid to semi-arid climatic conditions, which prevailed during the upper Olenekian and Middle Triassic, were conducive to the formation rather than the solution of evaporites. However, episodes of a more humid climate during deposition of the succession are documented by the intercalations of terrigenous sediments and the levels of surface karst (Jaglarz and Szulc, 2003; Jaglarz and Hryniewicz, 2014). In spite of the lack of any direct evidence for the dissolution of evaporites by fresh water (e.g., meteoric cements), one can assume that the solution-collapse breccias were formed during recurrent episodes of sediment emersion, as a result of karstification, due to the percolation of fresh waters. The effect of this is the reddish (comprising oxidized iron compounds) matrix of the breccias. Near-surface diagenesis under fresh-water conditions is further evidenced by dedolomites containing calcite pseudomorphs after sulphates (Myophoria Beds; Jaglarz and Rychliński, 2010) and by the remains of oomoldic porosity (in the Middle Triassic dolomitized calcarenites; Jaglarz, 2012).

CONCLUSIONS

The upper Olenekian–Ladinian carbonate succession of the Tatra Mts comprises dolostone breccias of solution-collapse origin.

The breccias originated during episodes of cyclic sediment emersion as a result of gradual sediment collapse after the dissolution of intercalated evaporites. Karst phenomena were related to short periods of pluvialisation.

The processes that preceded breccia formation included the precipitation of evaporites as well as the early-diagenetic dolomitization of lime muds.

The diagenetic processes, which postdated breccia formation, in the order of their occurrence, were: cementation of the breccia by sulphates, dolomitization of the breccia matrix, the dissolution of sulphate cements, precipitation of the dolomite cements and the void-filling dolomites (i.e., in moulds after dissolved sulphate crystals), and finally chemical compaction.

Fracturing of the breccias (or even their rebrecciation) was a result of later tectonic processes.

Acknowledgements

Kind permission for the field work was provided by the Authority of the Tatra National Park in Zakopane. The authors were supported by the Jagiellonian University DS funds. P.J. was supported by MNiSW Grant 2P04D05229. We would like to thank Tadeusz Peryt (Polish Geological Institute – National Research Institute), two anonymous reviewers and Michał Gradziński (journal editor) for their critical and helpful comments and suggestions which greatly improved the final version of the manuscript.

REFERENCES

Adams, A. E. & MacKenzie, W. S., 1998. *A Colour Atlas of Carbonate Sediments and Rocks Under the Microscope.* Manson Publishing, London, 180 pp.

Adams, A. E., MacKenzie, W. S. & Guilford, C., 1984. *Atlas of Sedimentary Rocks Under the Microscope.* Longman Group UK Ltd, Harlow, 104 pp.

Al-Juboury, A. J. & Ďurovič, V., 1996. Supratidal origin of Carpathian Keuper dolostones, *Mineralia Slovaca,* 28: 12–20.

Amthor, J. E. & Friedman, G. M., 1991. Dolomite-rock textures and secondary porosity development in Ellenburger Group carbonates (Lower Ordovician), west Texas and southeastern New Mexico. *Sedimentology*, 38: 343–362.

Andrusov, D., Bystrický, J. & Fusán, O., 1973. Outline of the structure of the West Carpathians. In: *X Congress of Carpathian-Balkan Geological Association. Introductory Excursion Guidebook.* Geologický Ústav Dionýza Štúra, Bratislava, 45 pp.

Bac-Moszaszwili, M., 1995. Diversity of Neogene and Quaternary tectonic movements in the Tatra Mountains. *Folia Quatenaria*, 66: 131–144.

Bac-Moszaszwili, M., Burchardt, J., Głazek, J., Iwanow, A., Jaroszewski, W., Kotański, Z., Lefeld, J., Mastella, L., Ozimkowski, W., Roniewicz, P., Skupiński, A. & Westwalewicz-Mogilska, E., 1979. *Geological Map of the Polish Tatra Mts. 1:30 000*. Wydawnictwa Geologiczne, Warszawa.

Bathurst, R. G., 1975. *Carbonate Sediments and their Diagenesis.* Elsevier, Amsterdam, 675 pp.

Beales, F. W. & Hardy, J. L., 1980. Criteria for recognition of diverse dolomite types with an emphasis on studies on host rocks Mississippi Valley-type ore deposits. In: Zenger, D. H., Dunham, J. B. & Ethington, R. L. (eds), *Concepts and Models of Dolomitization. Society of Economic Paleontologists and Mineralogists, Special Publication*, 28: 197–213.

Blount, D. N. & Moore, C. H., 1969. Depositional and non-depositional carbonate breccias, Chianthia quadrangle, Guatemala. *Bulletin of the Geological Society of America*, 80: 429–442.

Boggs, S. & Krinsley, D., 2006. *Application of Cathodoluminescence Imaging to the Study of Sedimentary Rocks*. Cambridge University Press, New York, 176 pp.

Burchart, J., 1968. Rubidium-strontium isochron ages of the crystalline core of the Tatra Mountains, Poland. *American Journal of Sciences,* 266: 895–907.

Dumont, T., Wieczorek, J. & Bouillin, J. P., 1996. Inverted Mesozoic rift structures in the Polish Western Carpathians (High-Tatric units). Comparison with similar features in the Western Alps. *Eclogae Geologicae Helvetiae*, 89: 181–202.

Dżułyński, S. & Gradziński, R., 1960. Source of the Lower Triassic clastics in the Tatra Mts. *Bulletin de l`Académie Polonaise des Sciences*, 8: 45–48.

Eliassen, A. & Talbot, M. R., 2005. Solution-collapse breccias of the Minkinfjellet and Wordiekammen Formations, Central Spitsbergen, Svalbard: a large gypsum palaeokarst system. *Sedimentology*, 52: 775–794.

Friedman, G. M., 1997. Dissolution-collapse breccias and paleokarst resulting from dissolution of evaporite rocks, especialy sulfates. *Carbonates and Evaporites*, 12: 53–63.

Fuglewicz, R., 1979. Megaspores found in the earliest Triassic deposits of Tatra Mts. *Rocznik Polskiego Towarzystwa Geologicznego*, 49: 271–275.

Gaetani, M., *et al.* (40 co-authors)*,* 2000. Early Ladinian. In: Dercourt, J., Gaetani, M., Vrielynck, B., Barrier, E., Biju-Duval, B., Brunet, M. F., Cadet, J. P., Crasquin, S. & Sandulescu, M. (eds), *Atlas Peri-Tethys. Palaeogeographical Maps.* CCGM/CGMW, Paris.

Gregg, J. M. & Sibley, D. F., 1984. Epigenetic dolomitization and the origin of xenotopic dolomite texture. *Journal of Sedimentary Petrology*, 54: 908–931.

Jaglarz, P., 2007. *Evolution of the Tatricum Basin in Late Olenekian Norian Time in the Polish Tatra Mts*. Unpublished PhD Thesis, Jagiellonian University in Krakow, 188 pp. [In Polish, with English summary.]

Jaglarz, P., 2010. Facies and sedimentary environment of the carbonate-dominated Carpathian Keuper from the Tatricum domain: results from the Dolina Smytnia valley (Tatra Mts, Southern Poland). *Annales Societatis Geologorum Poloniae*, 80: 147–161.

Jaglarz, P., 2012. Multi-stage dolomitization in the Lower–Middle Triassic succession of the High-Tatric series (Western Tatra Mts., Poland). *Przegląd Geologiczny*, 60: 284–293. [In Polish, with English summary.]

Jaglarz, P. & Hryniewicz, K., 2014. Skały węglanowe triasu dolnego (olenek górny). In: Jach, R., Rychliński, T. & Uchman, A. (eds), Sedimentary Rocks of the Tatra Mountains. Tatrzański Park Narodowy − Wydawnictwa, Zakopane, pp. 42–48. [In Polish.]

Jaglarz, P. & Rychliński, T., 2010. Remarks on nomenclature of the Triassic carbonate rocks from the Tatra Mts. *Przegląd Geologiczny*, 58: 327–334. [In Polish, with English summary.]

Jaglarz, P. & Szulc, J., 2003. Middle Triassic evolution of the Tatricum sedimentary basin: an attempt of sequence stratigraphy to the Wierchowa Unit in the Polish Tatra Mts. *Annales Societatis Geologorum Poloniae*, 73: 169–182.

Jaglarz, P. & Uchman, A., 2010. A hypersaline ichnoassemblage from the Middle Triassic carbonate ramp of the Tatricum domain in the Tatra Mountains, Southern Poland. *Palaeogeography, Palaeoclimatology, Palaeoecology*, 292: 71–81.

Janák, M., 1994. Variscan uplift of the crystalline basement, Tatra Mts., Central Western Carpathians: evidence from $^{40}Ar/^{39}Ar$ laser probe dating of biotite and P-T-t paths. *Geologica Carpathica,* 45: 293–300.

Jurewicz, E., 2003. Multistage evolution of the shear zone at the base of the Giewont Unit Polish Tatra Mts. *Geologica Carpathica*, 54: 337–351.

Jurewicz, E., 2005. Geodynamic evolution of the Tatra Mts. and the Pieniny Klippen Belt (Western Carpathians): problems and comments. *Acta Geologica Polonica*, 55: 295–338.

Jurewicz, E. & Słaby, E., 2004. The Zadnie Kamienne "ravenous" shear zone (High-Tatric Nappe) – conditions of deformation. *Geological Quarterly*, 48: 371–382.

Karakitsios, V. & Pomoni-Papaioannou, F., 1998. Sedimentological study of the Triassic solution-collapse breccias of the Ionian Zone (NW Greece). *Carbonates and Evaporites*, 13: 207–218.

Kotański, Z., 1954. Tentative genetical classification of breccias on the basis of studies concerning the High-Tatric Trias in the Tatra Mountains. *Rocznik Polskiego Towarzystwa Geologicznego*, 24: 63–116. [In Polish, with English summary.]

Kotański, Z., 1956. High-Tatric Campilian in the Tatr Mts. *Acta Geologica Polonica*, 6: 65–73. [In Polish, with English summary.]

Kotański, Z., 1959a. Stratigraphical sections of the High-Tatric series in the Tatra Mts. *Biuletyn Instytutu Geologicznego*, 139: 7–139. [In Polish, with English summary.]

Kotański, Z., 1959b. Stratigraphy, sedimentology and paleogeography of the High-Tatric Triassic in the Tatra Mts. *Acta Geologica Polonica*, 9: 113–145.

Kotański, Z., 1961. Tectogénese et reconstitution de la paléogeografie de la zone haut-tatrique dans les Tatras. *Acta Geologica Polonica*, 11: 186–476. [In Polish, with French summary.]

Leszczyński, S. & Pszonka, J., 2014. Skały klastyczne triasu dolnego (?ind–olenek dolny). In: Jach, R., Rychliński, T. & Uchman, A. (eds), *Sedimentary Rocks of the Tatra Mountains*. Tatrzański Park Narodowy −Wydawnictwa, Zakopane, pp. 34−41. [In Polish.]

Łuczyński, P., 2002. Depositional evolution of the Middle Jurassic carbonate sediments in the High-Tatric succession, Tatra Mountains, Western Carpathians, Poland. *Acta Geologica Polonica*, 52: 365–378.

Machel, H. G., 2000. Application of cathodoluminesce to carbonate diagenesis. In: Pagel, M., Barbin, V., Blanc, P. & Ohnenstetter, D. (eds), *Cathodoluminesce in Geosciences*. Springer-Verlag, New York, pp. 271–301.

Machel, H. G., 2004. Concept and models of dolomitization: a critical reappraisal. In: Braithwaite, C. J. R., Rizzi, G.

& Darke, G. (eds), *The Geometry and Petrogenesis of Dolomite Hydrocarbon Reservoirs. Geological Society, London, Special Publications*, 235: 7–63.

Michalík, J., 1993. Mesozoic tensional basins in the Alpine-Carpathian shelf. *Acta Geologica Hungarica*, 36: 395–403.

Michalík, J., 1994. Notes on the paleogeography and paleotectonics of the Western Carpathian area during the Mesozoic. *Mitteilungen der Österreichischen Geologischen Gesellschaft*, 86: 101–110.

Middleton, G. V., 1961. Evaporite solution breccias from the Mississippian of Southwest Montana. *Journal of Sedimentary Petrology*, 31: 189–195.

Miller, J., 1988. Cathodoluminescence microscopy. In: Tucker, M. (ed.), *Techniques in Sedimentology*. Blackwell Science, Oxford, pp. 174–190.

Mišík, M. & Jablonský, J., 2000. Lower Triassic quartzites of the Western Carpathians: transport directions, source of clastics. *Geologica Carpathica*, 51: 251–264.

Morrow, D. W., 1982. Descriptive field classification of sedimentary and diagenetic breccia fabrics in carbonate rocks. *Bulletin of Canadian Petroleum Geology*, 30: 227–229.

Pomoni-Papaioannou, F. & Carotsieris, Z., 1993. Dolomitizaton patterns in Jurassic-Cretaceous dissolution-collapse breccias of Mainalon Mountain (Tripolis Unit, Central Peloponnesus-Greece). *Carbonates and Evaporites*, 8: 9–22.

Pomoni-Papaioannou, F. & Karakitsios, V., 2002. Facies analysis of the Trypali carbonate unit (Upper Triassic) in central-western Crete (Greece): an evaporite formation transformed into solution-collapse breccias. *Sedimentology*, 49: 1113–1132.

Radke, B. M. & Mathis, R. L., 1980. On the formation and occurrence of saddle dolomite. *Journal of Sedimentary Petrology*, 50: 1149–1168.

Ren, M. & Jones, B., 2018. Genesis of island dolostones. *Sedimentology*, 65: 2003–2033.

Roniewicz, P., 1966. Lower Werfenian (Seisian) clastics in the Tatra Mts. *Acta Geologica Polonica*, 16: 1–90. [In Polish, with English summary.]

Roniewicz, P., 1969. Sedimentation of the Nummulite Eocene in the Tatra Mts. *Acta Geologica Polonica*, 19: 503–608. [In Polish, with English summary.]

Rychliński, T., Ivanova, D. K, Jaglarz, P. & Bucur, I. I., 2013. Benthic foraminifera and calcareous algae from the Anisian−Norian succession in the Tatras (Poland and Slovakia): New data from High-Tatric and Krížna units. *Studia Universitatis Babeş-Bolyai, Geologia*, 58: 21−43.

Rychliński, T. & Jaglarz, P., 2017. An evidence of tectonic activity in the Triassic of the Western Tethys: a case study from the carbonate succession in the Tatra Mountains (S Poland). *Carbonates and Evaporites*, 32: 103–116.

Rychliński, T., Jaglarz, P. & Uchman, A., 2014. Unusually well preserved casts of halite crystals: A case from the Upper Frasnian of northern Lithuania. *Sedimentary Geology*, 308: 44–52.

Scholle, P. A., Stemmerik, L., Ulmer-Scholle, D., Di Liegro, G. & Henk, F. H., 1993. Paleokarst-influenced depositional and diagenetic patterns in Upper Permian carbonates and evaporites, Karstryggen area, central East Greenland. *Sedimentology*, 40: 895–918.

Shinn, E. A., 1968. Practical significance of birdseye structures in carbonate rocks. *Journal of Sedimentary Petrology,* 38: 215–223.

Sibley, D. F. & Gregg, J. M., 1987. Classification of dolomite rock textures. *Journal of Sedimentary Petrology*, 57: 967–975.

Simpson, F., 1988. Solution-generated collapse (SGC) structures associated with bedded evaporites: significance to base-metal and hydrocarbon localization. *Geoscience Canada*, 15: 89–93.

Soták, J., 2010. Paleoenvironmental changes across the Eocene-Oligocene boundary: insights from the Central Carpathian Paleogene Basin. *Geologica Carpathica*, 61: 393–418.

Spötl, C. & Pitman, J. K., 1998. Saddle (baroque) dolomite in carbonates and sandstones: A Reappraisal of a Burial-Diagenetic Concept. In: Morad, S. (ed.), *Carbonate Cementation in Sandstones: Distribution Patterns and Geochemical Evolution*. Blackwell Publishing Ltd., Oxford, pp. 437–460.

Swennen, R., Viaene, W. & Cornelissen, C., 1990. Petrography and geochemistry of the Belle Roche breccia (lower Visean, Belgium): evidence for brecciation by evaporite dissolution. *Sedimentology*, 37: 859–878.

Szulc, J., 2000. Middle Triassic evolution of the Northern Peri-Tethys area as influenced by early opening of the Tethys Ocean. *Annales Societatis Geologorum Poloniae*, 70: 1–48.

Veizer, J., 1970. Zonal arrangement of the Triassic rocks of the Western Carpathians: A contribution to the dolomite problem. *Journal of Sedimentary Petrology,* 40: 1287–1301.

Vogel, K., Muchez, P. & Viaene, W., 1990. Collapse breccias and sedimentary conglomerates in the Lower Visean of Vesdre area (E-Belgium). *Annales de la Société Géologique de Belgique*, 113: 359–371.

Wieczorek, J., 2000. Mesozoic evolution of the Tatra Mountains (Carpathians). *Mitteilungen der Gesellschaft der Geologie und Bergbaustudenten in Wien*, 44: 241–262.